scientific reports

Check for updates

OPEN

Radiation exposure induces genome-wide alternative splicing events in *Aedes aegypti* mosquitoes

Harley Bendzus-Mendoza[1], Amanda Rodriguez[2,3], Tathagata Debnath[1], C. Donovan Bailey[2], Hailey A. Luker[2,3] & Immo A. Hansen[2,3,4]✉

Sterile insect technique is a method to control insect pest populations by sterilizing males with ionizing radiation. However, radiation sickness lowers the fitness of sterilized males. In this study, we investigate impacts of ionizing radiation on gene transcription, specifically alternative splicing events in irradiated male *Aedes aegypti* mosquitoes. We compared RNA sequencing data from mosquitoes irradiated with a single standard X-ray dose of 50 Grey and un-irradiated control mosquitoes using the Multivariate Analysis of Transcript Splicing computational tool. We found that radiation exposure caused alternative splicing events in 197 genes that are involved in a variety of biological processes including the Hippo and Notch cell signaling pathways. Our results suggest that radiation damage produced by ionizing radiation can alter the splicing of genes involved in important biological functions in male *Ae. aegypti* mosquitoes. These findings identify several new leads for new projects aimed at understanding the impact of radiation-induced alternative splicing on mosquito fitness and improving sterile insect technique by the development of radio-resistant mosquito strains.

Keywords *Aedes aegypti*, Radiation, Differential spliced genes, Alternative splicing, rMATS

Aedes aegypti, the yellow fever mosquito, is the primary vector of several deadly diseases, including yellow fever, dengue fever, chikungunya, and Zika[1]. These insects are a major public health threat in many parts of the world, especially in tropical and subtropical regions[2,3]. *Ae. aegypti* are notorious for their ability to transmit diseases to humans causing widespread morbidity and substantial mortality[4]. Therefore, controlling their populations is crucial for public health and has become a major focus of research in years[5]. By reducing mosquito populations, the risk of disease transmission can be mitigated. There are several methods for controlling *Ae. aegypti* populations, including insecticide use, biological control methods, and community-based interventions[6]. Insecticides can be applied to kill adult mosquitoes and larvae, but overuse leads to the rapid development of resistance in mosquito populations[7].

An alternative method for controlling *Ae. aegypti* populations is the sterile insect technique (SIT). SIT is a method used to control the populations of insect pests, in which sterile males are released into the wild to mate with wild type females resulting in production of unfertilized eggs, over time reducing pest populations[3]. This technique has been used successfully in a variety of pest insect species, including the Mediterranean fruit fly and the screwworm fly[8,9]. SIT has been proven safe, effective, and environmentally friendly since it does not involve the use of pesticides. It is species-specific and does not make use of genetically modified organisms[10].

The use of ionizing radiation to sterilize male insects is the method of choice in many SIT programs[11]. This technique involves exposing male insects to a precise dose of ionizing radiation. The purpose of irradiating males is to damage DNA in the gametes, which causes permanent sterility[12]. Ionizing radiation causes ionization of the atoms and molecules within the cells, creating highly reactive free radicals that can damage DNA strands[13]. This damage can range from single-strand breaks to more severe double-strand breaks that can cause mutations or chromosomal abnormalities in the gametes[12]. Dosages between 5 and 300 Gy are used to completely sterilize different insect pest species with each species requiring different dosages for optimal results[14]. The dose needs to cause enough DNA damage to produce at least one dominant-lethal mutation in each of the gametes. The dosage cannot be so high that the target species are killed or immediately develop severe radiation sickness[15]. The optimal radiation dosage for sterilizing male *Ae. aegypti* has been previously determined to be 50 Gy[16].

[1]Department of Computer Science, New Mexico State University, Las Cruces, NM, USA. [2]Department of Biology, New Mexico State University, Las Cruces, NM, USA. [3]Molecular Vector Physiology Laboratory, New Mexico State University, Las Cruces, NM, USA. [4]Institute of Applied Biosciences, New Mexico State University, Las Cruces, NM, USA. ✉email: immoh@nmsu.edu

While irradiating mosquitoes with 50 Gy causes complete sterility, it still reduces male fitness and lifespan[17]. This is a problem because sterile males must successfully compete with wild males for SIT to be effective. To better understand the impact of radiation exposure on mosquitoes, we previously investigated changes in the transcriptome of irradiated male *Ae. aegypti*. We found dramatic changes in the transcriptome, specifically a robust up-regulation of the transcription of DNA repair genes involved in nucleotide-excision repair, interstrand cross-link repair, DNA strand elongation, and double strand break repair[18]. In the current study, we hypothesized that radiation induces distinct alternative splicing events (ASEs) in male *Ae. aegypti*. Alternative splicing plays a critical role in the regulation of gene expression in multicellular organisms[19]. This process allows the generation of multiple protein isoforms from a single gene[20]. ASEs can have a profound impact on the development, differentiation, and fitness of eukaryotes and have also been implicated as a source of phenotypic diversity in different multicellular organisms[21]. ASEs are an important component of the sex-determination pathway in many insects, including mosquitos[22,23].

The mechanisms of alternative splicing involve the selective inclusion or exclusion of specific exons, introns, or splice sites from pre-mRNA transcripts[24]. This process is mediated by the spliceosome, a large complex of ribonucleoproteins that recognizes and processes the pre-mRNA transcript[25]. Alternative splicing can be regulated by various factors and its effects can be diverse, ranging from no effect to changes in protein domains, subcellular localization, protein stability, and function[26]. Alternative splicing can also generate different protein isoforms with distinct tissue-specific expression patterns or temporal shifts during development, contributing to the complexity of eukaryotic gene expression.

The results of our analysis of our dataset confirmed our hypothesis that radiation-exposure triggers specific and significant ASEs in mosquitoes.

Materials and methods

Data retrieval

The transcriptomic data used in this study was retrieved from the National Library of Medicine – BioProject PRJNA895439 https://www.ncbi.nlm.nih.gov/bioproject/?term=PRJNA895439. From this data set of 16 samples, only 8 are used in this study. They are Non-irradiated 1 to 4 with accession numbers SRX18064883, SRX18064884, SRX18064887, SRX18064888, and Irradiated 1 to 4 for which the accession numbers are SRX18064873, SRX18064874, SRX18064875, SRX18064876.

Data analysis

The quality of the raw sequence data was assessed using FastQC v0.11.9[27], and adapter sequences were removed using Trimmomatic v.0.36[18,28]. The trimmed reads were used for this study and mapped to the most recent *Ae. aegypti* reference genome (AaegL5.3) found on Vectorbase using STAR v1.5.3 (CITATION). For detailed information on the number of reads per sample, average Mbase yield, quality scores and call accuracy for untrimmed RNA-seq data, please refer to Pinch et al.[18]. Alternative splicing events were detected by using the resulting BAM files from STAR as input to rMATS v4.1.2 analysis[29]. A false discovery rate (FDR) cutoff value of 0.05 and Delta Percent Spliced In (Δ PSI) values less than −0.1 and greater than 0.1 were used to determine significantly differential ASEs. The IncLevelDifference column from the rMATS output provided the Δ PSI values. Shashmi plots of all significant ASEs were generated by using rMATS output JCEC.txt files as input to rmats2sashimiplot v2.0.3[30]. Additional graphs were generated using R v3.6.3[31] and ggplot2 v3.3.6[32]. We selected genes that had ASEs that were statistically different between control and irradiated samples were selected for further GO and KEGG pathway analyses. The recommended thresholds for Δ PSI and FDR are 5% and 1% respectively[29]. We chose a Δ PSI threshold value of 10% for our dataset, for more stringent detection of ASE events.

GO analysis

All three Gene Ontology (GO) categories (biological process, cellular component, and molecular function) and their subsequent terms for the alternatively spliced genes (ASGs) were generated using DAVID v2023q4[33]. The ASGs were used as the query. The "Aedes aegypti" was used as the background in DAVID. All graphs visualizing the fold change value for all terms detected were automatically generated by ggplot2 version 3.5.0[32] package in the Rstudio version 1.4.1106 using R version 4.2.0[31].

The DAVID software uses the Fisher's Exact Test to determine if a set of genes from a user's list are significantly enriched for a specific GO term compared to the expected frequency based on the whole genome background, essentially comparing the observed gene count within a GO term to what would be expected by chance, using a 2×2 contingency table approach[54].

The null hypothesis states that there is no enrichment for the GO term in the user's gene list, meaning the distribution of genes within the GO term is random compared to the background genome.

The Fisher's Exact Test calculates a p-value based on the observed frequencies in the contingency table, indicating the probability of observing such an extreme distribution of genes within the GO term if the null hypothesis was true.

KEGG pathway analysis

The KEGG Pathway analysis was performed using DAVID v2023q4[33–36]. Genes with unique and significant ASEs identified by rMATS analysis were analyzed. The Functional Analysis was performed using the Entrez[33] gene IDs as queries and "Aedes aegypti" as background in DAVID. The KEGG Pathway results were downloaded as .txt file in tabular format and converted to .csv for further analysis. The results were visualized as graphs generated by ggplot2 version 3.5.0[32] package in the Rstudio version 1.4.1106 using R version 4.2.0[31].

Mosquito rearing and irradiation treatment

All mosquito cultures and irradiation treatments were performed as previously described by Pinch et al.[18]. Briefly, *Ae. aegypti* Liverpool strain mosquito eggs were obtained from BEI Resources[37] and maintained for at least four generations in the insectary at the Molecular Vector Physiology Laboratory at New Mexico State University. Eggs were hatched in deionized (DI) water and larvae were reared in groups of 250 individuals, fed *ad libitum* on cat food pellets. Pupae were placed in cages to emerge under standard rearing conditions (28 °C, 80% humidity, light: dark cycle of 14:10). After emergence, male mosquitoes were manually separated into cages with an aspirator and fed *ad libitum* on 20% sucrose solutions for 24 h, prior to irradiation[38]. Four groups of 30 male mosquitoes were irradiated with a 50 Gy dose of ionizing radiation using a MultiRad 350 instrument (Faxitron, Tucson, AZ). Four control groups of 30 male mosquitoes were placed in the X-ray cabinet for the same duration without being irradiated. After treatment, all groups were transferred to cages with access to 20% sucrose solution and were kept under standard rearing conditions for 24 h. For more details refer to Pinch et al.[18].

RNA extraction

Total RNA was extracted using the Qiagen RNeasy kit (Qiagen, Hilden, Germany) following the manufacturer's protocol. RNA concentrations were measured using a NanoDrop spectrophotometer (ThermoFisher, Waltham, MA) and the samples were stored at -80 °C.

RT-PCR

We selected two genes that had a significant occurrence of specific ASEs for RT-PCR analysis (see Table 1). These two genes showed high statistical evidence for the occurrence of one of two specific types of splicing events: alternative 3' splice sites (A3SS), and alternative 5' splice sites (A5SS). We developed primers for these genes. Actin primers used for a control were published previously[39] (Table 1). All the primers were designed using NCBI Primer-BLAST and ordered from Eurofins Genomics (Louisville, KY).

cDNAs were synthesized from the isolated RNA samples using iScript Reverse Transcription Supermix (Bio-Rad, Hercules, CA) following the manufacturer's protocol. A PCR was performed using a *Taq* 2x Master Mix (New England Biolabs, Ipswich, MA) following the manufacturer's protocol. PCR samples were then analyzed on 1.5% Agarose gels containing SYBR Safe DNA stain (Invitrogen, Waltham, MA). The gel images were then captured using the Omega Fluor Gel Documentation system (Thomas Scientific, Chadds Ford Township, PA).

Results

Quality check RNA-Seq analysis

All trimmed libraries contained an average of 14,250,430 reads per sample (Table 2). The percentage of uniquely mapped reads ranged from 70.20 to 78.62%, with an average of 74.41%. The percent of reads that were multi-mapped ranged from 13.56 to 20.79%, with an average of 17.72%. The average percent of reads mapped to multiple loci was 17.45%, and the average number of reads mapped to too many loci was 0.27% (Supplementary Table 1). No reads were unmapped due to too many mismatches. The average percentage of reads that were too short to be mapped to the reference genome was 7.84%. The average percentage of reads that were unmapped was less than 8% across all samples. Overall, these mapping quality metrics indicate that the RNA-seq data obtained in this study are of high quality and suitable for downstream analysis.

Alternative splicing events after irradiation

In total, we detected 15,016 ASEs among the transcriptomes of irradiated and non-irradiated mosquitoes (Supplementary Tables 2–6). 289 of these ASEs were significantly differentially alternatively spliced between both groups (FDR < 0.05 and Δ PSI (delta Percent Spliced In) values less than −0.1 and greater than 0.1), with 181 unique genes undergoing ASEs (Fig. 1).

Specifically, 88 events were classified as alternative 3' splice site events (A3SS), 104 as alternative 5' splice site events (A5SS), 17 as mutually exclusive exon events (MXE), 12 as retained intron (RI) events, and 68 as skipped exon events (SE) (Fig. 1c). All significant splicing event visualizations can be found in supplementary Figs. 1–5.

There was considerable variation in the Δ PSI values among the different types of splicing events (Fig. 2a). For A3SS events, the majority had Δ PSI values between −0.6 and 0.58. Similarly, the majority of all A5SS events had Δ PSI values between −0.55 and 0.69. Δ PSI values for RI and MXE, ranged between −0.2 and 0.61 and −0.81 to 0.41, respectively. SE events had Δ PSI value ranges more similar to that of A3SS and A5SS, with values ranging from −0.58 to 0.58. MXE events were found to have the smallest median Δ PSI value while A3SS events were

Gene Identifier – Primer Name	Primer Sequence
AAEL019921 - A3SS Forward	CGATACCGGGTAATTCGCCA
AAEL019921 - A3SS Reverse	AGTGCTCAAATCGGAGAGTAACA
AAEL012861 - A5SS Forward	GCTATCGGTGGTGATGAGGG
AAEL012861 - A5SS Reverse	CGATGACGGCTACGATGGAA
XM_001659913 - Actin Forward	GTCGGTGATGAGG
XM_001659913 - Actin Reverse	TCGTCGTATTCCT

Table 1. Primers for RT-PCR. Primer information for the A3SS gene, A5SS gene, and actin.

Input		Mapped		Multi-Mapped		Unmapped	
Treatment and Replicate	Number of input reads	Number of uniquely mapped reads	Percent of uniquely mapped reads	Total number of multi-mapped reads	Total percent multi-mapped reads	Total number of unmapped reads	Total percent unmapped reads
Non-irradiated, 1 Accession: SRX18064883	12,411,980	9,758,733	78.62%	1,683,163	13.56%	970,084	7.82%
Non-irradiated, 2 Accession: SRX18064884	15,923,200	11,409,923	71.66%	3,311,749	20.79%	1,201,528	7.55%
Non-irradiated, 3 Accession: SRX18064887	13,731,647	10,115,540	73.67%	2,766,648	20.15%	850,459	6.18%
Non-irradiated, 4 Accession: SRX18064888	19,519,586	13,701,967	70.20%	2,857,546	14.64%	29,522,073	15.16%
Irradiated, 1 Accession: SRX18064873	14,289,609	11,157,998	78.08%	2,416,360	16.91%	715,251	5.01%
Irradiated, 2 Accession: SRX18064874	12,995,141	9,365,871	72.07%	2,571,656	19.79%	1,057,614	8.14%
Irradiated, 3 Accession: SRX18064875	12,956,300	9,779,686	75.48%	2,182,151	16.84%	994,463	7.67%
Irradiated, 4 Accession: SRX18064876	12,175,978	9,189,854	75.48%	2,319,173	19.05%	666,951	5.47%
Averages	**14,250,430**	**10,559,947**	**74.41%**	**2,513,556**	**17.72%**	**4,497,303**	**7.88%**

Table 2. Mapping statistics. Mapping statistics generated by STAR for trimed RNA sequencing data are given for each treatment replicate. The table includes information on the input reads, number of uniquely mapped reads, percent of uniquely mapped reads, total number of multi-mapped reads, total percent multi-mapped reads, total number of unmapped reads, total percent unmapped reads, and averages for each.

found to have the highest median Δ PSI value. A5SS and RI events have observable bimodal distributions of Δ PSI values, while A3SS and SE events seemed to have less pronounced bimodal distributions. The kernel density for RI values was more pronounced than those of all other events. The wide fluctuations between − 0.5 and 0.4 suggests that RI events were more likely to have those Δ PSI values. Furthermore, the Δ PSI values were evenly distributed across both enhanced and repressed splice junctions, indicating that there was no bias towards either type of junction (Fig. 2b). All the different types of the ASE events had statistically significant (| Δ PSI |> 0.1) variation of Δ PSI events. This indicates that radiation exposure triggers every type of ASEs. The distribution of the Δ PSI values in the violin plots (Fig. 2a) indicate statistically significant changes after radiation exposure."

The genes that undergo significant ASEs after irradiation were mapped to the three chromosomes of Ae. aegypti (Fig. 2c). We found that all five ASEs occurred genome wide. A5SS splicing events were the most common type of ASE occurring to genes across all chromosomes, accounting for 36% of all ASEs. A3SS events were the second most common occurring ASE observed, accounting for approximately 30% of all events. SE events were less frequent, accounting for approximately 23%, while MXE and RI events were the least common occurring ASEs both accounting for only 10% of all events. A5SS, A3SS, and SE events are evenly distributed among the three chromosomes. However, the significant MXE and RI events are less abundant in chromosome 1. Chromosome 2 has the most significant MXE events, while the chromosome 3 has most of the RI events occurring on them.

As previously described by Pinch et al.[18], 149 genes were significantly differentially expressed between the non-irradiated and irradiated *Ae. aegypti*. A cross-analysis of the DEGs from the previous study and the significantly ASGs shown here, identified 16 genes that were both significantly differentially expressed and alternatively spliced (Fig. 2d).

Functional analysis of radiation-induced ASGs

The functional analysis of the significantly ASGs revealed that these genes are involved in various biological processes and molecular functions (Fig. 3). The identified biological processes associated with these ASGs, include actin filament binding, thiol-dependent deubiquitinase, ubiquitin-like protein-specific protease activity, deubiquitinase activity, omega peptidase activity, actin binding, calcium ion binding, cytoskeletal protein binding, phosphotransferase activity, kinase activity, and transferase activity (Fig. 3a). The molecular functions that were found to be associated with the ASGs, include nucleotide biosynthetic processes, nucleoside phosphate

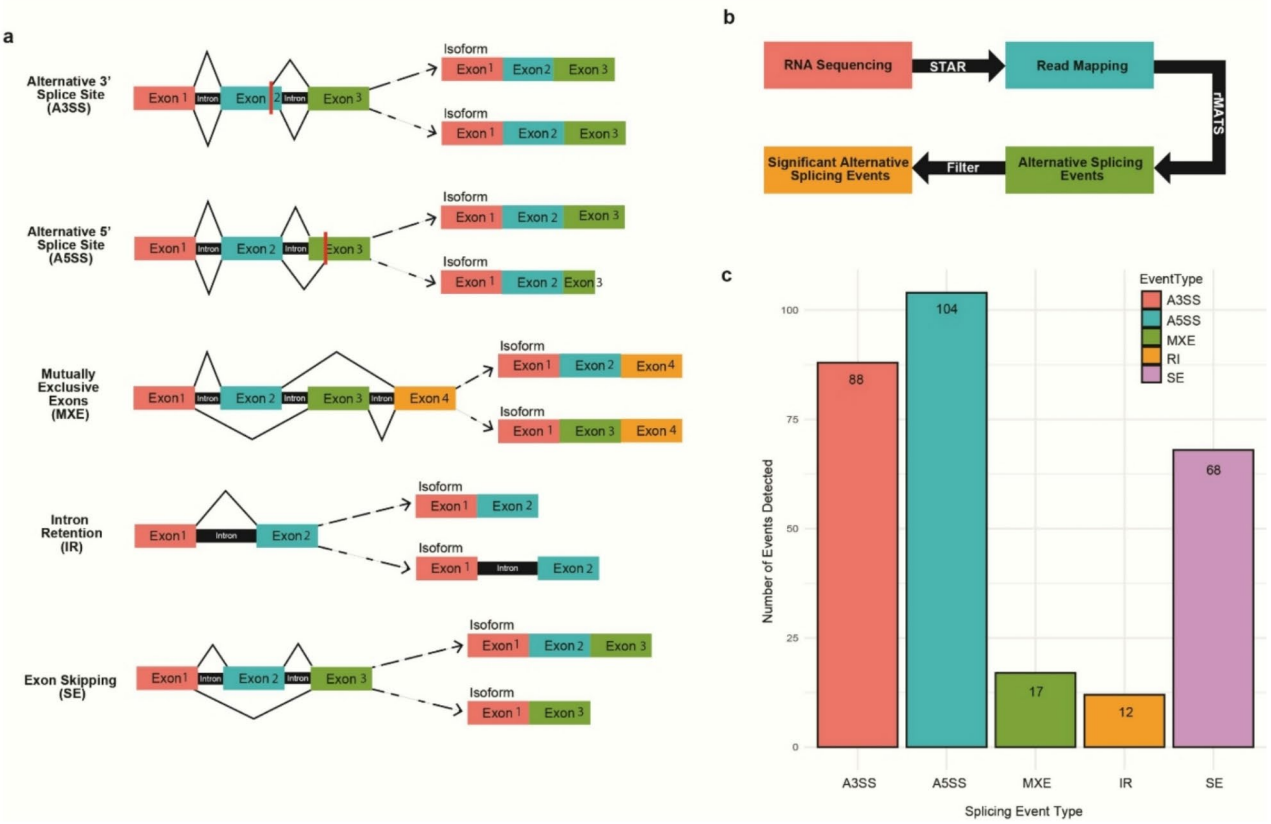

Fig. 1. Differential alternative splicing events induced by radiation exposure. (**a**) A schematic diagram that depicts five different ASE that were identified using rMATS, along with the various mature RNA isoforms that can result from each event. (**b**) Schematic diagram visualizing the bioinformatics workflow for data processing. The filter is representative of an FDR < 0.5 and |ΔPSI| > 0.1 for ASE. (**c**) A bar graph showing the number of significant ASE for each event type (FDR < 0.5 and |ΔPSI| > 0.1).

biosynthetic processes, intracellular signal transduction, organophosphate metabolic processes, phosphorylation, phosphate-containing compound metabolic processes, phosphorus metabolic processes, signal transduction, response to stimulus, regulation of cellular processes, and biological regulation (Fig. 3b).

Figure 4 shows the results from a KEGG Pathway analysis of genes with irradiation-induced ASEs. Among the identified pathways, the HIPPO signaling pathway, Purine metabolism, and Notch signaling pathway emerged as the most abundant. These pathways play crucial roles in various cellular processes such as signal transduction, response to stimuli, and regulation of cellular activities[44–46].

Confirmation of radiation-induced A3SS and A5SS events via RT-PCR analysis

We performed RT-PCR on RNA samples from unirradiated control mosquitoes and mosquitoes 24 h after irradiation. Figure 5 shows agarose gels loaded with RT-PCR products and a schematic diagram of the targeted ASG and the location of the primers used for PCR. Different sized PCR products between control and experimental groups depict ASEs in these genes.

Discussion

The effect of radiation-induced ASEs is an emerging area of research, with important implications for both basic biology, applied biomedical research, and arthropod pest control[40,41]. Here, we investigate the impact of ionizing radiation on the alternative splicing patterns in male *Ae. aegypti*.

Gene expression changes in multicellular organisms can take hours, days, or even weeks to become apparent, depending on the nature and severity of the stressor/stimulus and the specific genes involved[42]. Differential gene expression and alternative splicing patterns may vary over time as the cells adapt to the stressor or undergo different phases of the stress response[43]. For this study, we chose to analyze the transcriptomes of whole mosquitoes 24 h after irradiation and compare those to the transcriptomes of un-irradiated control mosquitoes, in order to identify significant ASEs. This whole-body-transcriptomics approach was designed to detect common ASEs that occur in all tissues and not tissue-specific ASEs. There is a variety of alternative splicing types/patterns in eukaryotes[44], and we identified five different types of splicing events in our dataset: A3SS, A5SS, MXE, RI, and SE. Of these five, A3SS, A5SS, and SE are by far the most prevalent after irradiation treatment. These three types of ASEs have been shown to be more prevalent in metazoan model organisms like *Caenorhabditis elegans*

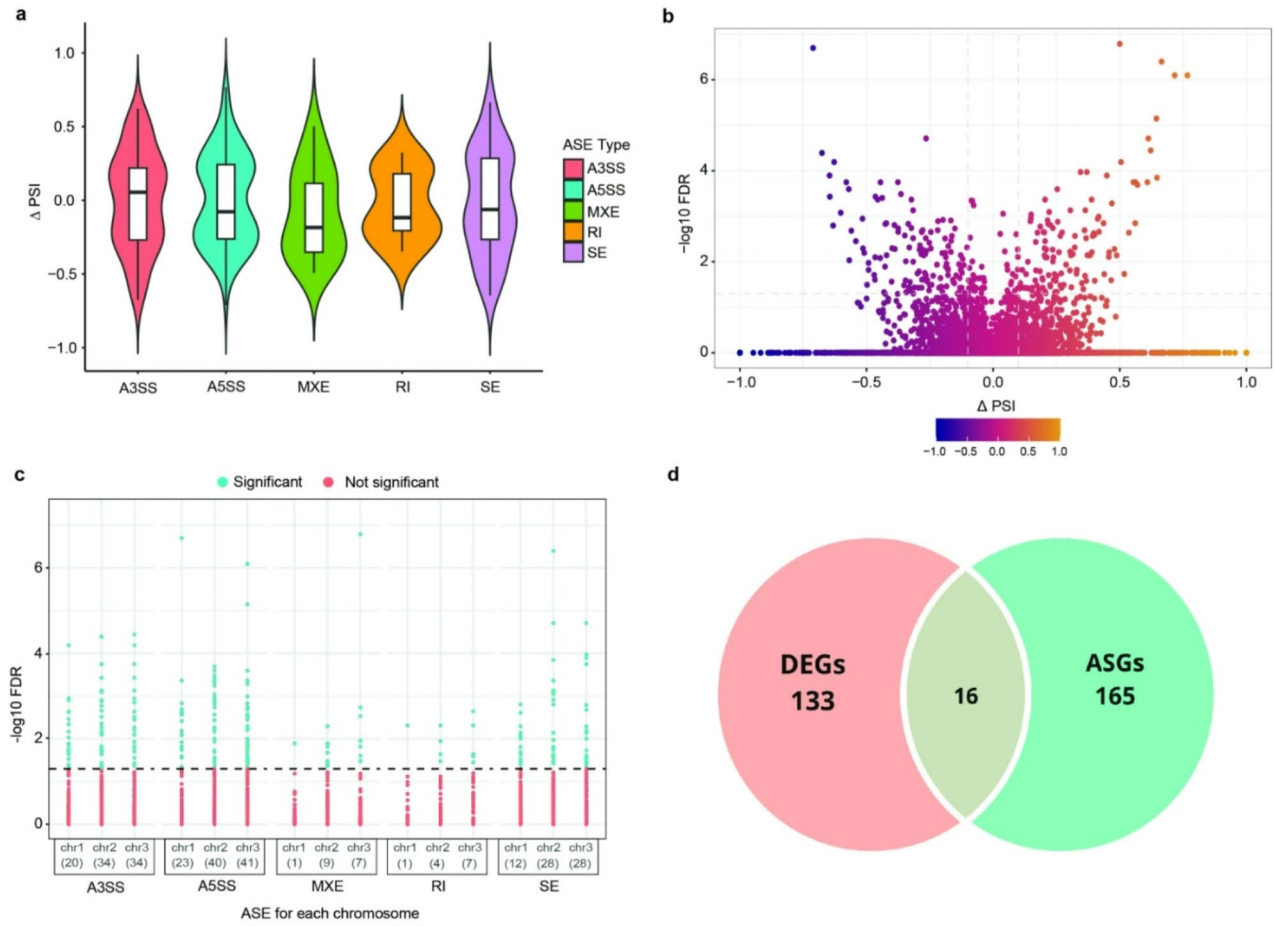

and *Drosophila melanogaster*[45]. In the same study, it was suggested that intron retention is the rarest type of ASE in metazoan eukaryotes. In support of this notion, we found that RI is indeed the rarest type of ASE in our *Ae. aegypti* dataset.

Ae. aegypti has three pairs of chromosomes with a homomorphic sex chromosome[46]. Genes that underwent ASEs after radiation-exposure were mapped to all three chromosomes revealing that these irradiation-induced ASEs occur genome wide. *Ae. aegypti* has over 15,000 predicted genes[47], 298 of these genes were either differentially expressed or alternatively spliced and 16 were both, after irradiation. These results suggest that there are roughly three hundred genes that are radiation-responsive, and that these genes either undergo changes in expression or in splicing but only a undergo both.

The functional analysis of DEGs after irradiation, identified in the previous study by Pinch et al.[17], revealed a diverse array of biological processes associated with these radiation responsive genes. Our functional analysis of ASGs occurring after irradiation identified a specific set of biological processes involving the regulation of

◀**Fig. 2**. Radiation induces genome-wide alternative splicing events. (**a**) Irradiation causes significant differences in specific ASE types. Shown are Violin plots displaying the distribution of ΔPSI values for statistically significant ASE (|ΔPSI| > 0.1 and FDR < 0.05) for each event type (A3SS, A5SS, MXE, RI, and SE). The symmetric curve in the plot is the kernel density, and the box represents the interquartile range, with the lower and upper bounds indicating the 25th and 75th percentile of the distribution, respectively. The horizontal line in the box represents the median, while the whiskers show the minimum and maximum values. (**b**) Irradiation causes significant differences in ASEs. Shown is a Volcano plot plotting 15,016 ASEs found in both, non-irradiated and irradiated mosquitoes. The data points in the plot are colored based on their ΔPSI values. Only the points outside the three dashed gray lines correspond to significantly different ASEs (|ΔPSI| > 0.1 and FDR < 0.05). (**c**) Radiation exposure results in significant ASEs occurring in genes from all chromosomes of *Ae. aegypti*. Dot plot showing all ASEs detected for each event type for each chromosome. All significant ASEs are shown in blue and occur above the dashed horizontal line (FDR < 0.05), while all non-significant ASEs are shown in red. The number of significant ASEs for each chromosome are shown underneath the chromosome number for each event type. (**d**) A small number of genes are both alternatively spliced and differentially expressed in irradiated mosquitoes. Shown is a Venn diagram displaying differentially expressed genes (DEGs) and alternatively spliced genes (ASGs) for irradiated mosquitoes.

ubiquitin signaling processes and cytoskeletal-related processes. Our analysis also identified a wide range of molecular functions associated with these ASGs. Three pathways were highly enriched in our KEGG pathway analysis. These were the Hippo signaling, Purine metabolism, and Notch signaling pathways. The Hippo signaling pathway is involved in the regulation of cell proliferation and apoptosis[48–50]. This pathway is conserved in metazoic eukaryotes and is associated with tumor growth, suppression, and resistance to radiation[51,52]. One of the alternatively spliced genes that we identified in this pathway is PP2A, which is part of a regulatory complex within the Hippo pathway[53]. The purine metabolism pathway regulates DNA repair, has been associated with cancer therapy, and implicated to promote radiation resistance[54,55]. The Notch signaling pathway, another conserved pathway involved in cell fate, has been associated with tumor cell proliferation, and radiation resistance[56,57]. An important regulator protein, NCSTN[58], is also alternatively spliced upon radiation exposure.

In conclusion, we have identified a list of genes that are differentially alternatively spliced in irradiated *Ae. aegypti* males. Our findings clearly show that ionizing radiation does significantly impact the regulation of gene alternative splicing. A detailed functional analysis of the different isoforms of the ASGs detected in this study, will reveal a subset of putative proteins important for radiation resistance in cancers and irradiated mosquitoes for SIT. Considering the fast opportunities opened up by CRISPR/Cas9-mediated gene editing in mosquitoes, this information could ultimately lead to the development of radio-resistant mosquito strains with improved performance in sterile-insect-technique. While difference in splicing regulation between different species are not uncommon[59], our research provides a foundation for better understanding cellular responses to radiation in multicellular organisms. Radiation-induced alternative splicing mechanisms may aid the development of novel approaches in cancer research, and pest control.

Fig. 3. Gene Ontology terms of alternatively spliced genes. Bar graph representing the -log10(p.value) for gene ontology (GO) terms within each GO domain (Biological Process, Cellular Component, and Molecular Function). Each bar represents a GO term and is color-coded according to the domain it is encompassed by. The length of each bar represents the-log10(p.value) for the GO terms within their respective domains. The y-axis displays the different GO terms, while the x-axis represents the -log10(p.value) values.

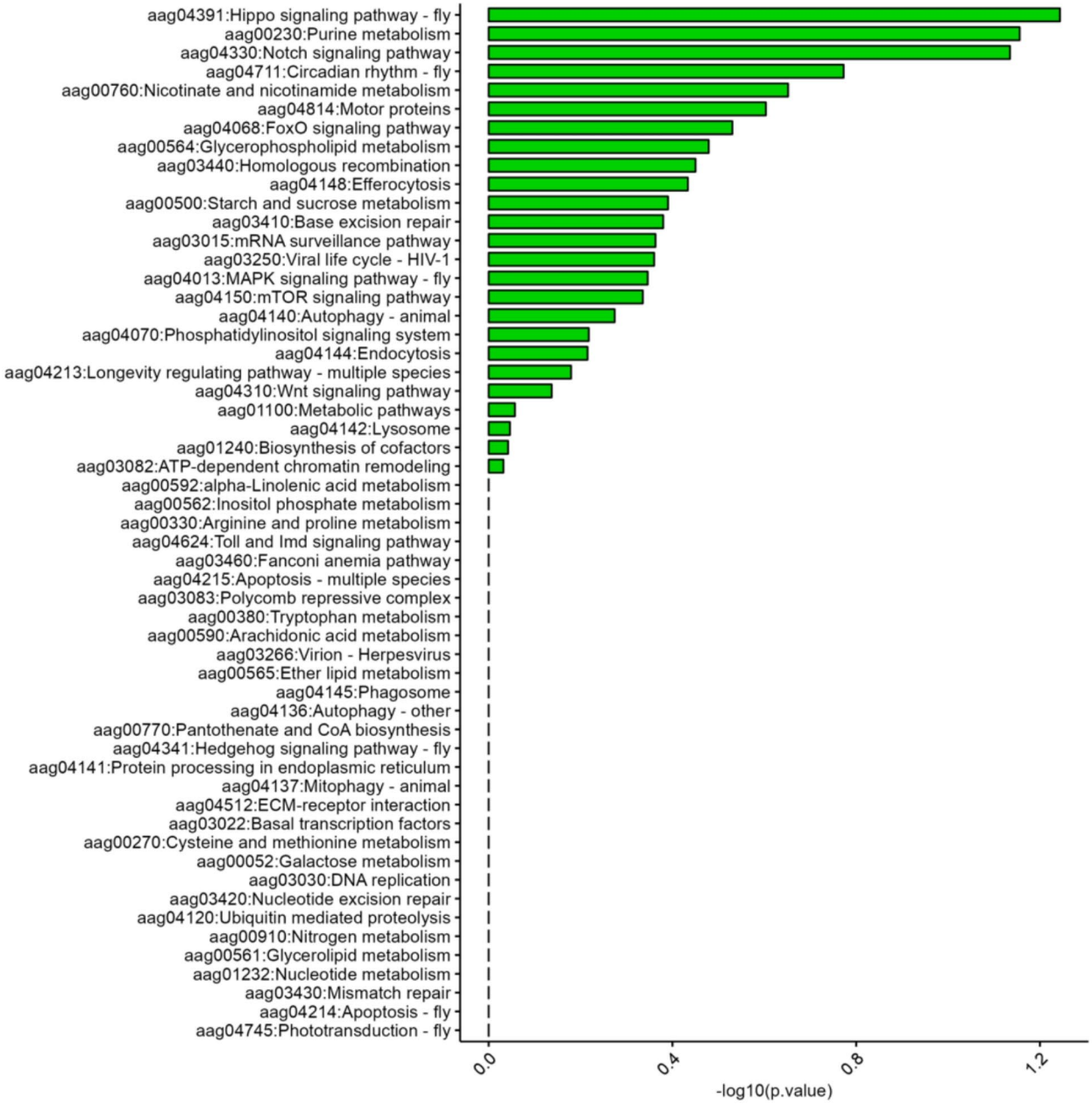

Fig. 4. KEGG Pathway enrichment analysis of genes with irradiation-induced alternatively spliced events. Shown are KEGG Pathways that alternately spliced genes that occur after irradiation are involved in. The -log10(p.value) is displayed on the x-axis.

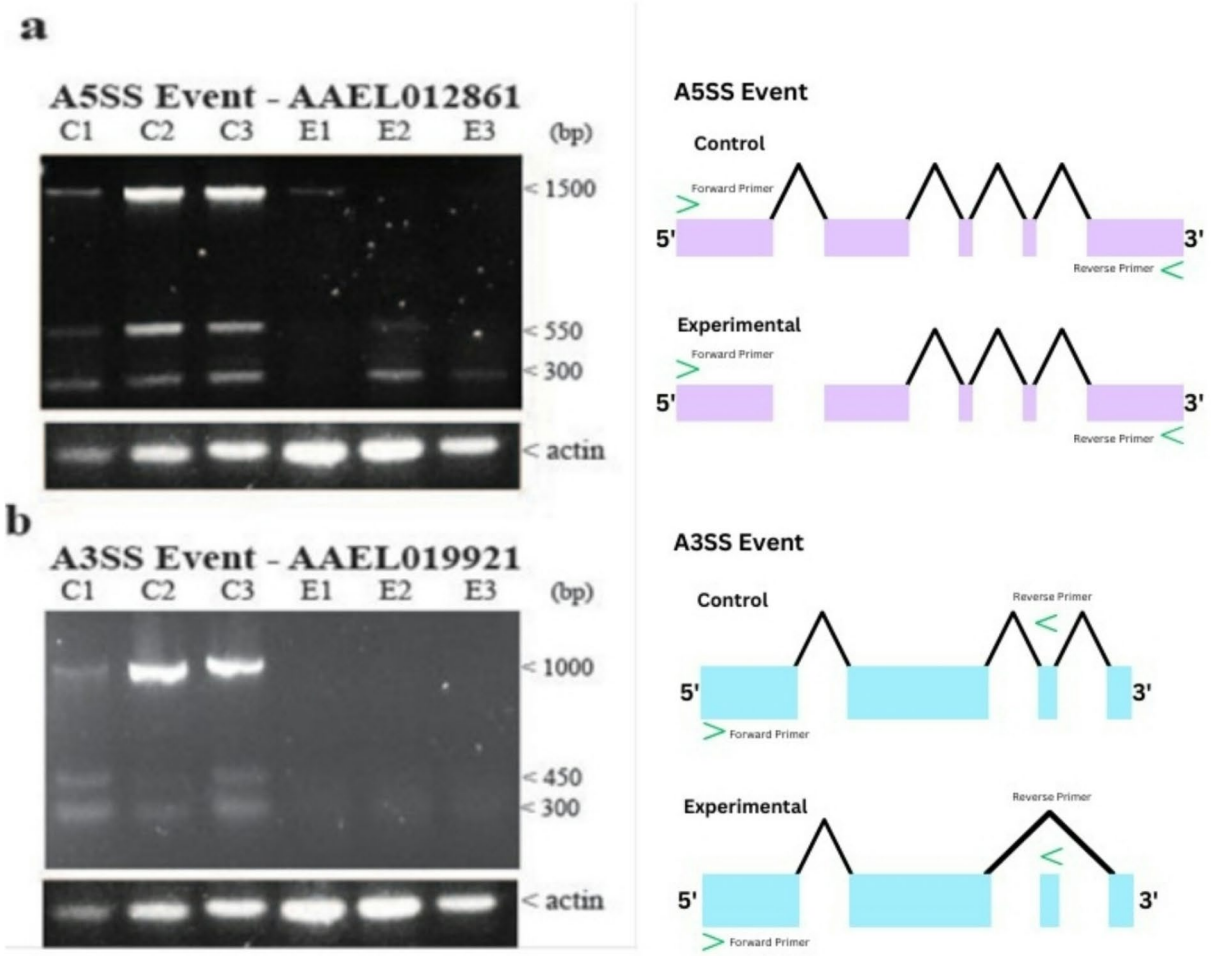

Fig. 5. Confirmation of radiation-induced A3SS and A5SS events via RT-PCR analysis. Shown are RT-PCR gels (left) and the location of the primer target sequence on the targeted gene (right). (**a**) An A5SS alternative splicing event of the gene AAEL012861 upon radiation treatment. Three control samples (C1, C2, C3) are loaded on the left of the experimental groups (E1, E2. E3). The actin panel was used as a loading control. Note the absence of the 1500 bp RT-PCR fragments in the irradiated groups. The position of the primers (green arrow heads) used for this experiment and the proposed A5SS alternative splicing pattern of AAEL012861 is shown in the right panel. (**b**) An A3SS alternative splicing event of AAEL019921 upon radiation treatment. The loading pattern is identical to that shown above and the same actin control panel was used. Note the absence of the 1000 bp RT-PCR fragment in the irradiated groups. Splicing patterns of this event and location of primers (green arrow heads) is shown in the right panel.

Data availability

The transcriptomics datasets used in this study were produced by Pinch et al.[18]. These datasets are publicly available and can be accessed from the Gene Expression Omnibus (GEO) database under the accession number PRJNA895439 at https://www.ncbi.nlm.nih.gov/bioproject/?term=PRJNA895439. Further information on the datasets and their processing can be found in the publication by Pinch et al.[18].

Received: 19 June 2024; Accepted: 14 March 2025
Published online: 24 March 2025

References

1. Souza-Neto, J. A., Powell, J. R. & Bonizzoni, M. Aedes aegypti vector competence studies: A review. *Infect. Genet. Evol.* **67**, 191–209 (2019).
2. Andrew, J. & Bar, A. Morphology and morphometry of *Aedes aegypti* adult mosquito. *Annual Res. Rev. Biology* 52–69 (2013).
3. Bourtzis, K. & Vreysen, M. J. B. Sterile Insect Technique (SIT) and Its Applications. *Insects* 12, (2021).

4. Socha, W., Kwasnik, M., Larska, M., Rola, J. & Rozek, W. Vector-Borne viral diseases as a current threat for human and animal health-One health perspective. *J. Clin. Med.* **11**, (2022).
5. Wilder-Smith, A. et al. Epidemic arboviral diseases: priorities for research and public health. *Lancet. Infect. Dis.* **17**, e101–e106 (2017).
6. Weeratunga, P., Rodrigo, C., Fernando, S. D. & Rajapakse, S. Control methods for *Aedes albopictus* and *Aedes aegypti*. *The Cochrane Database of Systematic Reviews* (2017).
7. Jangir, P. K. & Prasad, A. Spatial distribution of insecticide resistance and susceptibility in *Aedes aegypti* and *Aedes albopictus* in India. *Int. J. Trop. Insect Sci.* **42**, 1019–1044 (2022).
8. The Gamma Ray. And the elimination of the screwworm fly in Curacao. *Am. J. Public. Health Nations Health* **45**, 1162–1163 (1955).
9. Shooing the screwworm fly. *Sci. (New York N Y* **253**, 28 (1991).
10. Alphey, L. et al. Sterile-insect methods for control of mosquito-borne diseases: an analysis. *Vector Borne Zoonotic Dis.* **10**, 295–311 (2010).
11. Bakri, A., Mehta, K. & Lance, D. R. in *Sterile Insect Technique*. chap. Chapter 9, pp. 233–268. (2005).
12. Helinski, M. E., Parker, A. G. & Knols, B. G. Radiation biology of mosquitoes. *Malar. J.* **8** (Suppl 2), S6 (2009).
13. Reisz, J. A., Bansal, N., Qian, J., Zhao, W. & Furdui, C. M. Effects of ionizing radiation on biological molecules–mechanisms of damage and emerging methods of detection. *Antioxid. Redox Signal.* **21**, 260–292 (2014).
14. Bakri, A., Mehta, K. & Lance, D. Sterilizing insects with ionizing radiation. *Sterile insect technique: principles and practice in area-wide integrated pest management.* 233–268 (2005).
15. Bond, J. G. et al. Optimization of irradiation dose to *Aedes aegypti* and *Ae. albopictus* in a sterile insect technique program. *PLoS One* **14**, e0212520 (2019).
16. Chen, C. et al. Developing the radiation-based sterile insect technique (SIT) for controlling Aedes aegypti: identification of a sterilizing dose. *Pest Manag. Sci.* **79**, 1175–1183 (2023).
17. Rodriguez, S. D. et al. The effect of the radio-protective agents ethanol, trimethylglycine, and beer on survival of X-ray-sterilized male Aedes aegypti. *Parasites Vectors*. **6**, 211 (2013).
18. Pinch, M., Bendzus-Mendoza, H. & Hansen, I. A. Transcriptomics analysis of ethanol treatment of male *Aedes aegypti* reveals a small set of putative radioprotective genes. *Front. Physiol.* **14**, (2023).
19. Wang, Y. et al. Mechanism of alternative splicing and its regulation. *Biomed. Rep.* **3**, 152–158 (2015).
20. Matlin, A. J., Clark, F. & Smith, C. W. Understanding alternative splicing: towards a cellular code. *Nat. Rev. Mol. Cell Biol.* **6**, 386–398 (2005).
21. Wright, C. J., Smith, C. W. & Jiggins, C. D. Alternative splicing as a source of phenotypic diversity. *Nat. Rev. Genet.* **23**, 697–710 (2022).
22. Salz, H. K. Sex determination in insects: a binary decision based on alternative splicing. *Curr. Opin. Genet. Dev.* **21**, 395–400 (2011).
23. Biedler, J. & Tu, Z. *In Advances in Insect Physiology*. vol. 51, pp. 37–66. (Elsevier, 2016).
24. Lee, Y. & Rio, D. C. Mechanisms and regulation of alternative Pre-mRNA splicing. *Annu. Rev. Biochem.* **84**, 291–323 (2015).
25. House, A. E. & Lynch, K. W. Regulation of alternative splicing: more than just the ABCs. *J. Biol. Chem.* **283**, 1217–1221 (2008).
26. Zhu, L. Y., Zhu, Y. R., Dai, D. J., Wang, X. & Jin, H. C. Epigenetic regulation of alternative splicing. *Am. J. Cancer Res.* **8**, 2346–2358 (2018).
27. Andrews, S. vol. 2023. (2010).
28. Bolger, A. M., Lohse, M. & Usadel, B. Trimmomatic: a flexible trimmer for illumina sequence data. *Bioinformatics* **30**, 2114–2120 (2014).
29. Shen, S. et al. rMATS: robust and flexible detection of differential alternative splicing from replicate RNA-Seq data. *Proc. Natl. Acad. Sci.* **111**, E5593–E5601 (2014).
30. Xie, Z. vol. 2023. (2015).
31. Core Team, R. R. R: A language and environment for statistical computing. (2013).
32. Wickham, H. ggplot2: Elegant Graphics for Data Analysis. Springer-Verlag, New York. ISBN 978-3-319-24277-4. (2016).
33. Ge, S. X., Jung, D. & Yao, R. ShinyGO: a graphical gene-set enrichment tool for animals and plants. *Bioinformatics* **36**, 2628–2629 (2020).
34. Kanehisa, M., Furumichi, M., Sato, Y., Matsuura, Y. & Ishiguro-Watanabe, M. KEGG: biological systems database as a model of the real world. *Nucleic Acids Res.* **53**, D672–D677 (2025).
35. Kanehisa, M. Toward Understanding the origin and evolution of cellular organisms. *Protein Sci.* **28**, 1947–1951 (2019).
36. Kanehisa, M. & Goto, S. KEGG: Kyoto encyclopedia of genes and genomes. *Nucleic Acids Res.* **28**, 27–30 (2000).
37. Molestina, R. E. BEI resources: a biological resource center for parasitologists. *Trends Parasitol.* **26**, 559 (2010).
38. Rodriguez, S. D. et al. The effect of the radio-protective agents ethanol, trimethylglycine, and beer on survival of X-ray-sterilized male *Aedes aegypti*. *Parasites Vectors* **6**, 1–8 (2013).
39. Mitra, S. et al. Olfaction-Related gene expression in the antennae of female mosquitoes from common Aedes aegypti laboratory strains. *Front. Physiol.* 1367 (2021).
40. Sciarrillo, R. et al. The role of alternative splicing in cancer: from oncogenesis to drug resistance. *Drug Resist. Updates* **53**, 100728 (2020).
41. Koukidou, M. & Alphey, L. Practical applications of insects' sexual development for pest control. *Sex. Dev.* **8**, 127–136 (2014).
42. Alberts, B. et al. An overview of gene control. *Molecular Biology of the Cell. 4th edition* (2002).
43. Fulda, S., Gorman, A. M., Hori, O. & Samali, A. Cellular stress responses: cell survival and cell death. *Int. J. Cell. Biol.* **214074** 2010 (2010).
44. Kim, E., Goren, A. & Ast, G. Alternative splicing: current perspectives. *Bioessays* **30**, 38–47 (2008).
45. Kim, E., Magen, A. & Ast, G. Different levels of alternative splicing among eukaryotes. *Nucleic Acids Res.* **35**, 125–131 (2007).
46. Nene, V. et al. Genome sequence of Aedes aegypti, a major arbovirus vector. *Sci. (New York N Y.* **316**, 1718–1723 (2007).
47. Waterhouse, R. M., Wyder, S. & Zdobnov, E. M. The Aedes aegypti genome: a comparative perspective. *Insect Mol. Biol.* **17**, 1–8 (2008).
48. Misra, J. R. & Irvine, K. D. The Hippo signaling network and its biological functions. *Annu. Rev. Genet.* **52**, 65–87 (2018).
49. Aqeilan, R. Hippo signaling: to die or not to die. *Cell. Death Differ.* **20**, 1287–1288 (2013).
50. Huang, J., Wu, S., Barrera, J., Matthews, K. & Pan, D. The Hippo signaling pathway coordinately regulates cell proliferation and apoptosis by inactivating yorkie, the drosophila homolog of YAP. *Cell* **122**, 421–434 (2005).
51. Zeng, Y. et al. CDK5 activates Hippo signaling to confer resistance to radiation therapy via upregulating TAZ in lung cancer. *Int. J. Radiation Oncology* Biology* Phys.* **108**, 758–769 (2020).
52. Sebé-Pedrós, A., Zheng, Y., Ruiz-Trillo, I. & Pan, D. Premetazoan origin of the Hippo signaling pathway. *Cell. Rep.* **1**, 13–20 (2012).
53. Ribeiro, P. S. et al. Combined functional genomic and proteomic approaches identify a PP2A complex as a negative regulator of Hippo signaling. *Mol. Cell* **39**, 521–534 (2010).
54. Yin, J. et al. Potential mechanisms connecting purine metabolism and cancer therapy. *Front. Immunol.* **9**, 1697 (2018).
55. Zhou, W. et al. Purine metabolism regulates DNA repair and therapy resistance in glioblastoma. *Nat. Commun.* **11**, 3811 (2020).
56. Capaccione, K. M. & Pine, S. R. The Notch signaling pathway as a mediator of tumor survival. *Carcinogenesis* **34**, 1420–1430 (2013).

57. Theys, J. et al. High NOTCH activity induces radiation resistance in Non small cell lung cancer. *Radiother. Oncol.* **108**, 440–445 (2013).
58. Li, H. et al. NCSTN promotes hepatocellular carcinoma cell growth and metastasis via β-catenin activation in a Notch1/AKT dependent manner. *J. Experimental Clin. Cancer Res.* **39**, 1–18 (2020).
59. Barbosa-Morais, N. L. et al. The evolutionary landscape of alternative splicing in vertebrate species. *Sci. (New York N Y)* **338**, 1587–1593 (2012).

Author contributions

HBM, AR, TD contributed to the project by annotating and analyzing RNA-seq data, producing figures and tables, performing statistical analyses, and co-writing the manuscript. IH, DB, HL developed the experiments and co-wrote the manuscript.

Declarations

Competing interests

The authors declare no competing interests.

Additional information

Supplementary Information The online version contains supplementary material available at https://doi.org/10.1038/s41598-025-94529-6.

Correspondence and requests for materials should be addressed to I.A.H.

Reprints and permissions information is available at www.nature.com/reprints.

Publisher's note Springer Nature remains neutral with regard to jurisdictional claims in published maps and institutional affiliations.